

# Cortical Damping: Analysis of Thalamocortical Response Transformations in Rodent Barrel Cortex

David J. Pinto\*, Jed A. Hartings\*<sup>1</sup>, Joshua C. Brumberg<sup>2</sup>, Daniel J. Simons<sup>1</sup>

Department of Neuroscience, Brown University, Providence, RI 02912, <sup>1</sup>Department of Neurobiology, University of Pittsburgh, Pittsburgh, PA 15261 and <sup>2</sup>Department of Psychology, Queens College, Flushing, NY 11367, USA

**In the whisker-barrel system, layer IV excitatory neurons respond preferentially to high-velocity deflections of their principal whisker, and these responses are inhibited by deflections of adjacent whiskers. Thalamic input neurons are amplitude and velocity sensitive and have larger excitatory and weaker inhibitory receptive fields than cortical neurons. Computational models based on known features of barrel circuitry capture these and other differences between thalamic and cortical neuron response properties. The models' responses are highly sensitive to thalamic firing synchrony, a finding subsequently confirmed in real barrels by *in vivo* experiments. Here, we use dynamic systems analysis to examine how barrel circuitry attains its sensitivity to input timing, and how this sensitivity explains the transformation of receptive fields between thalamus and cortex. We find that strong inhibition renders the net effect of intracortical connections suppressive or *damping*, distinguishing it from previous amplifying models of cortical microcircuits. In damping circuits, recurrent excitation enhances response tuning not by amplifying responses to preferred inputs, but by enabling them to better withstand strong inhibitory influences. Dense interconnections among barrel neurons result in considerable response homogeneity. Neurons outside the barrel layer respond more heterogeneously, possibly reflecting diverse networks and multiple transformations within the cortical output layers.**

## Introduction

Seminal neurophysiological studies have provided evidence that the receptive field properties of cortical cells in layer IV are determined directly by the receptive fields of their thalamic input neurons (Hubel and Wiesel, 1962). The existence of extensive interconnections among cortical neurons suggests, however, that local circuit processing also shapes receptive fields (White and Rock, 1980; Benshalom and White, 1986; Ahmed *et al.*, 1994). Anatomically, layer IV is distinct for its abundance of spiny stellate cells, small excitatory neurons that have locally ramifying dendrites and axons (Calloway 1998; Petersen and Sakmann, 2001). The number of connections among these cells probably exceeds those of thalamocortical synapses, which represent only a small proportion of the total number of excitatory synapses within layer IV (White and DeAmicas, 1977; White 1978; White and Rock, 1981).

An extensive network of interconnected excitatory neurons represents a positive feedback system that can confer highly non-linear transforming properties onto the constituent circuits. Accordingly, considerable theoretical attention has been directed toward understanding the role of positive feedback in the processing of afferent signals by layer IV circuitry. A number of computational models have incorporated these and other common elements of cortical circuitry into a 'canonical' microcircuit. Previous models of cat visual cortical circuitry, for example, employ positive feedback provided by recurrent excitatory connections to enhance response selectivity by amplifying responses to thalamic inputs associated with preferred stimuli

(Douglas *et al.*, 1989, 1995; Douglas and Martin, 1991; Ben-Yishai *et al.*, 1995; Somers *et al.*, 1995; Suarez *et al.*, 1995; Adorjan *et al.*, 1999) [reviewed by Ferster and Miller (Ferster and Miller, 2000)].

Here we examine the role of local intracortical connections in another experimentally well-characterized system, the thalamocortical circuit that processes tactile information from facial whiskers in rodents. Layer IV of the primary somatosensory cortex contains whisker-related clusters of synaptically interconnected neurons, called 'barrels', that receive the vast majority of their inputs from corresponding groups of neurons in the thalamus, called 'barreloids' (Woolsey and Van der Loos, 1970; Chmielowska *et al.*, 1989). Physiologically, both thalamic and cortical neurons respond robustly, yet somewhat differently, to relatively simple sensory stimuli in the form of individual whisker deflections (Simons and Carvell, 1989). In this paper, we review differences in thalamic and cortical receptive field properties that define the thalamocortical response transformation. We then describe how essential principles of barrel organization are implemented in two computational models. Simulation results confirm the sufficiency of these principles in explaining barrel neuron responses and, further, provide an avenue for in-depth analysis of the circuit's function.

As in visual cortical circuits, responses of layer IV barrel neurons appear to be determined by the temporal interplay between direct thalamocortical excitation and strong, locally generated cortical inhibition (Miller *et al.*, 2001). In particular, we find that strong feedforward and feedback inhibition render the net effect of intracortical connections *damping*, in contrast to models of the canonical microcircuit. Recurrent excitation contributes prominently to cortical response selectivity, however, by enabling responses evoked by preferred stimuli to withstand momentarily the pervasive effects of intra-barrel inhibition. These dynamics render both simulated and real barrel circuits highly sensitive to the firing synchrony of thalamic barreloid neurons, a property which may distinguish processing by damping versus amplifying circuitry.

## What Do Barrels Do?

### *Thalamocortical Response Transformation*

Layer IV of rodent somatosensory cortex contains anatomically distinct neuronal aggregates, called barrels, that correspond in one-to-one fashion with individual whiskers on the rat's face (Woolsey and Van der Loos, 1970; Welker 1971). Barrels contain at least two principal neuronal populations, excitatory spiny neurons and inhibitory smooth neurons. The two populations are synaptically connected reciprocally to each other and recurrently to themselves. Both receive afferent input from thalamocortical neurons (White, 1989; Keller, 1995). Neurons within a barrel are also related functionally in that each responds

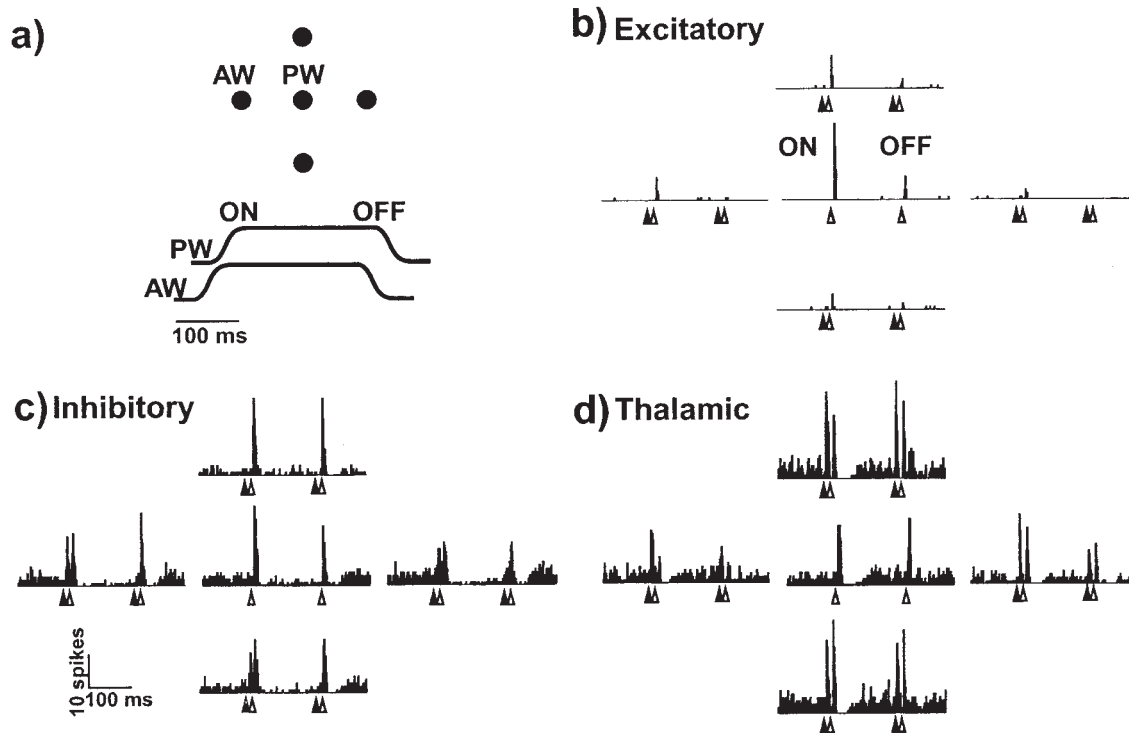


**Figure 1.** Transformation of receptive fields between thalamus and barrel cortex. Panel (a) shows a schematic of ramp-and-hold whisker deflection applied to the principal whisker (PW) and each of the four adjacent whiskers (AW). Panels (b)–(d) present peristimulus time histograms (PSTHs) from an excitatory barrel neuron (b), inhibitory barrel neuron (c) and thalamic neuron (d). In each case, the central PSTH shows responses to 40 repetitions of deflecting the PW in the direction that elicits the most spikes. Surrounding PSTHs show responses to paired AW–PW deflections, with the AW deflection starting 20 ms prior to PW deflection. AWs were deflected randomly in eight directions. Arrows indicate stimulus onset (ON) and offset (OFF): closed arrows, AW; open arrows PW.

most robustly to deflection of the same principal whisker (PW) [for review see (Simons, 1997; Miller *et al.*, 2001)].

To understand the transformation of receptive fields between thalamus and cortex in the whisker system, Simons and Carvell (Simons and Carvell, 1989) examined the responses of three types of neurons to the same ramp-and-hold whisker deflection stimuli (Fig. 1). The three populations included thalamic input neurons and both regular and fast spike neurons in the cortical barrel (Simons, 1978); the latter are believed to correspond to spiny excitatory and smooth inhibitory neurons, respectively. Figure 1a presents a schematic of the whisker deflections used in their study. Figure 1b–d show peristimulus time histograms (PSTHs) from representative excitatory (b), inhibitory (c) and thalamic (d) neurons generated in response to 40 stimulus repetitions. In each case, the center PSTH shows the neuron's response to PW deflection while the surrounding PSTHs show responses to deflections of each of the four immediately adjacent whiskers (AWs) followed 20 ms later by deflection of the PW.

By comparing responses of the thalamic input neuron to those of the cortical barrel neurons, several differences in response properties between thalamus and cortex become apparent. These receptive field transformations will be referred to as RFT1–RFT4. First (RFT1), the level of background activity is significantly lower among excitatory cortical neurons as compared to thalamic neurons. Second (RFT2), in excitatory neurons, the transient response to the onset of principal whisker deflection (ON) is much greater than the response to deflection offset (OFF), in contrast to thalamic neurons for which ON and OFF responses have similar magnitude. This aspect of the response

transformation will be the focus of much of the following analysis. Third (RFT3), unlike thalamic neurons, excitatory neurons respond only weakly to deflection of AWs. That is, receptive fields of excitatory neurons in cortex are more spatially focused on the PW than those of their thalamic input neurons. Fourth (RFT4), also unlike thalamic neurons, excitatory neurons' responses to PW deflection are strongly suppressed when preceded by deflection of an AW. That is, receptive fields of excitatory neurons in cortex exhibit stronger surround inhibition than those of thalamic neurons. For all four properties, the receptive fields of inhibitory cortical neurons are qualitatively the same as thalamic input neurons; inhibitory cortical neurons display high levels of background activity, comparable ON versus OFF responses, spatially broad receptive fields, and comparatively weak levels of surround inhibition.

Based on these findings as well as a number of anatomical and functional results reported by others, Simons and Carvell (Simons and Carvell, 1989) hypothesized that the thalamo-cortical response transformation (RFT1–RFT4) results from processing within a single cortical barrel and emerges from four principles of barrel organization. First, individual excitatory and inhibitory barrel neurons differ in their nonlinear intrinsic response properties. For instance, inhibitory barrel neurons are able to discharge at high frequencies (McCormick *et al.*, 1985) and are thought to respond more linearly to input as compared to excitatory neurons (Angulo *et al.*, 1999). Second, thalamic neurons send convergent monosynaptic input onto *both* excitatory and inhibitory barrel neurons (White, 1978; Agmon and Connors, 1991; Swadlow and Gustav, 2000). Third, there is a network of synaptic connections among and between barrel

neurons of both types (Gibson *et al.*, 2000; Petersen and Sakmann, 2001) [for review see (Miller *et al.*, 2001)]. Fourth, inhibitory neurons are more responsive to input than excitatory neurons (Simons, 1978; Swadlow, 1995; McCasland and Hibbard, 1997). A major goal of the analysis presented below is to explain how the thalamocortical response transformation (RFT1–RFT4) emerges from these four principles.

### Computational Modeling

To test the hypothesis of Simons and Carvell, Kyriazi and Simons (Kyriazi and Simons, 1993) constructed a computational model of a whisker barrel based on the above four principles of barrel organization (Fig. 2a). The model consists of 100 barrel neurons, 70 excitatory ( $V_k^e$ ) and 30 inhibitory ( $V_k^i$ ). Each neuron is represented as a leaky linear integrator that describes membrane voltage. Figure 2c presents the equation describing the membrane voltage of an excitatory neuron; the equation for inhibitory neurons is similar. The generation of action potentials is governed in stochastic fashion using nonlinear voltage-to-firing rate probability functions  $P_e(V)$ ,  $P_i(V)$ . Both the firing rate functions and time constants are distinct for each of the two populations; the voltage-to-firing rate function is more linear for inhibitory versus excitatory neurons and the synaptic decay time constant for excitation ( $\tau_e$ ) is faster than for inhibition ( $\tau_i$ ) (see Appendix). Membrane voltages are determined by the spatial and temporal summation of synaptic events received from thalamic input neurons and from other excitatory and inhibitory neurons in the network. The ratio of excitatory to inhibitory neurons, the number of synapses received by each neuron (i.e. convergence: *ec*, *ic*, *tc*) and the relative strength of each type of synapse is based on estimates made from previously published light and electron microscopy studies [summarized by White (White, 1989); see also Keller (Keller, 1995)]. In the model, the mean strength of thalamic synapses onto inhibitory neurons ( $w_{ii}$ ) is set greater than that onto excitatory neurons ( $w_{ie}$ ), and the mean strength of inhibitory synapses ( $w_{ie}$ ,  $w_{ii}$ ) is set greater than that of excitatory synapses ( $w_{ee}$ ,  $w_{ei}$ ). Both factors contribute to the dominance of inhibition in the barrel circuit and, as described in the analysis below, both play major roles in the decoding of thalamic input signals by barrel circuitry.

Several innovative simulation strategies were introduced in the model of Kyriazi and Simons. First, input to the model barrel takes the form of spike trains recorded previously from real thalamic neurons in response to ramp-and-hold whisker deflections ( $PSTH_k$ ). Thus, model cortical neurons are made to respond to the same thalamic input as real cortical neurons, allowing for direct and quantitative comparisons of real and simulated responses. Second, the parameter values of the model are adjusted so that simulated responses match quantitatively with a small subset of responses from the real system, particularly the magnitude of ON and OFF responses. Remarkably, once the model is tuned to match these few selected data points (i.e. RFT2), all other aspects of the thalamocortical response transformation are quantitatively captured as well (i.e. RFT1, RFT3, RFT4) (Kyriazi *et al.*, 1996).

Beginning from the model of Kyriazi and Simons, Pinto *et al.* (Pinto *et al.*, 1996) derive a reduced computational model of the same system (Fig. 2b). A major goal of the reduced model is to incorporate the same principles of barrel organization within a minimal computational framework while retaining the capacity for both qualitative and quantitative comparisons with real data. Rather than representing activity of individual neurons, the equations of the reduced model describe the average activity in the excitatory and inhibitory cortical populations, reducing the

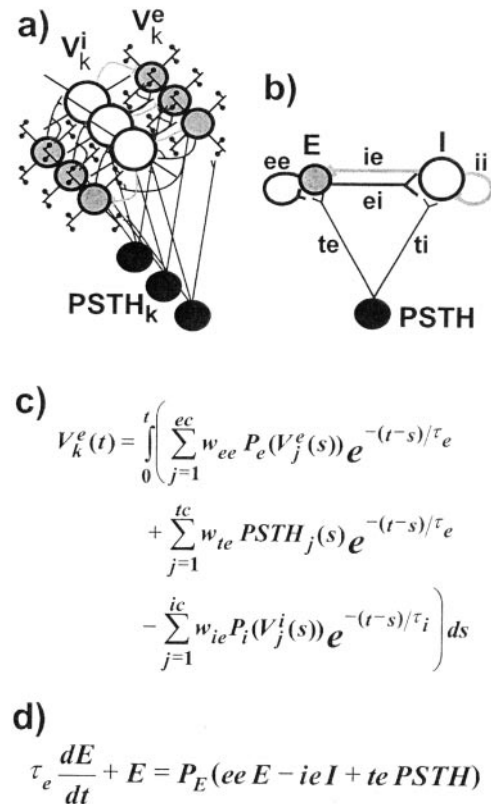


**Figure 2.** Computational models of the barrel circuit. Panels (a) and (b) present schematics of the full and reduced model barrel circuit as described in the text. Panels (c) and (d) present equations describing the membrane voltage of an excitatory neuron in the full model ( $V_k^e$ ) and the average activity in the excitatory population ( $E$ ) of the reduced model, respectively. Equations for inhibitory neurons and populations ( $V_k^i$ ,  $I$ ) are similar (see Appendix). The parameters and their values are defined in the text and Appendix.

system from over 100 equations to only two. Figure 2d presents the equation describing activity in the excitatory population; the equation for the inhibitory population is similar (see Appendix). Parameter values that do not come directly from the derivation are adjusted, as with the full model, so that simulated responses match quantitatively a small subset of responses from the real system, particularly the ON and OFF response magnitudes. Thalamic input to the reduced model takes the form of population responses accumulated from the entire set of pre-recorded thalamic neurons ( $PSTH$ ). The responses of the reduced model match quantitatively those of both the full model and real barrel populations. Importantly, as detailed below, the simple form of the reduced model allows for an analytic investigation of how the response transformation occurs that is not possible with the full model.

### Experimental Predictions and Validation

Both the full and reduced barrel models lead to numerous insights and specific predictions regarding the mechanisms of barrel processing. For instance, both models represent activity within a single cortical barrel yet capture all four aspects of the thalamocortical response transformation, including the emergence of strong surround inhibition. This is consistent with the hypothesis of Simons and Carvell (Simons and Carvell, 1989) that surround inhibition results from strong AW activation of inhibitory but not excitatory neurons within a single barrel and does not require horizontal interactions between neighboring

barrels. This hypothesis was tested experimentally in a study by Goldreich *et al.* (Goldreich *et al.*, 1999) in which ablation of the barrel corresponding to an AW has no effect on the level of surround inhibition in the barrel corresponding to the PW.

Another prediction arises from examining ON versus OFF responses in both real and simulated systems. Figure 3a presents population PSTHs of responses to whisker deflection onset and offset from both thalamic neurons and excitatory barrel neurons. Differences between the population ON and OFF response in cortex are probably due to some difference between those same responses in thalamus. One possibility is that barrel circuitry is sensitive to the slightly larger magnitude of the thalamic ON versus OFF response and responds by enhancing the difference in total spike count. A second possibility is that barrel circuitry is sensitive to the change in initial firing synchrony, i.e. faster onset rate, of the thalamic ON versus OFF response and responds by transforming this difference in population response timing into a difference in response magnitude.

To distinguish between these possibilities, the reduced model was presented with a battery of simulated ‘thalamic’ input triangles that were varied systematically in both magnitude and onset rate. Fast versus slow onset rates were used to approximate abrupt versus gradual changes in firing synchrony among thalamic input neurons. As illustrated in Figure 3b and quantified in Figure 3c, simulated excitatory barrel population responses are highly sensitive to the onset rate of thalamic input and less sensitive to input magnitude. The prediction, therefore, is that the responses of real excitatory barrel neurons are more sensitive to thalamic population input timing than to magnitude, and that this sensitivity explains the greater difference in size between the ON and OFF responses in cortex.

To test the prediction experimentally, Pinto *et al.* (Pinto *et al.*, 2000) examined responses of excitatory barrel neurons and thalamic neurons to whisker deflections having different velocities and amplitudes. These stimuli were used because they were found to evoke thalamic responses that varied in both timing and magnitude. Greater whisker deflection velocities evoke thalamic population responses having markedly faster onset rates, while thalamic population response magnitude increases slightly with either deflection velocity or amplitude. The early phase of thalamic local field potentials (LFPs), which presumably reflect synchronous firing among thalamic neurons, display a similar sensitivity to deflection velocity (Temereanca *et al.*, 2000). Thalamic population responses reflect those of trigeminal ganglion neurons which also encode deflection velocity in terms of their initial firing rates (Shoykhet *et al.*, 2000). Importantly, this temporal code for velocity is transformed by cortical circuitry, for the first time in the whisker-barrel pathway, into a code based on response magnitude. That is, increasing deflection velocities evoke abrupt increases in firing synchrony among thalamic neurons and, consistent with the models’ prediction, increasing response magnitudes from the cortical barrel. Changes in deflection amplitude do not affect thalamic firing synchrony and hence evoke only small changes in the cortical response.

The sensitivity of the cortical response to thalamic input timing is a robust feature of barrel processing. Figure 4 presents experimental response data from both thalamus and cortex obtained using a variety of whisker deflection protocols, including deflection onsets of different velocities and amplitudes, PW and AW deflection onsets, short and long plateau deflection offsets, and the initial response to sinusoidal deflections at different frequencies. The data were collected from experiments performed by five sets of investigators over the past

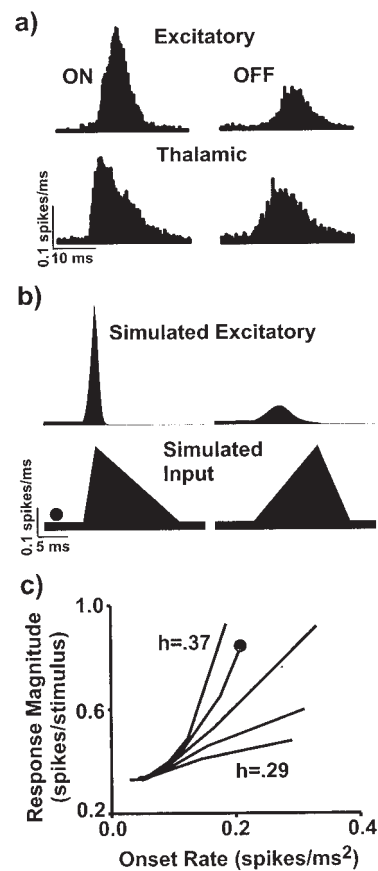


**Figure 3.** Sensitivity to input timing versus magnitude in simulated barrels. Panel (a) presents population PSTHs of ON and OFF responses accumulated from 68 excitatory barrel neurons and 64 thalamic neurons (Kyriazi *et al.*, 1994). Panel (b) presents examples of the reduced model’s response to simulated thalamic input triangles having different onset rates. Panel (c) quantifies the reduced model’s response to a battery of input triangles having a 15 ms base, time-to-peak ranging from 1 to 10 ms, heights (*h*) ranging from 0.29 to 0.37 spikes/ms in 0.02 increments, and with background activity of 0.04 spikes/ms. Onset rate is calculated as the height divided by time-to-peak. Lines connect responses to inputs having the same height but different onset rates. The gray dot tracks the same stimulus through each panel and in following figures.

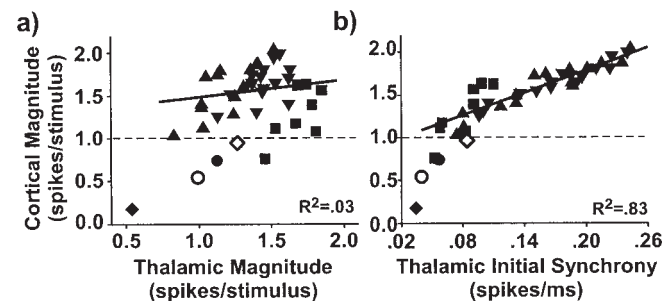


**Figure 4.** Sensitivity to input timing versus magnitude in real barrels. The symbols on both graphs indicate data averaged from populations of cortical and thalamic neurons in response to a variety of whisker deflection. These include onsets of deflections having different velocities and amplitudes [triangles (Pinto *et al.*, 2000)], PW and AW deflection onsets [open and closed diamond (Simons and Carvell, 1989; Bruno and Simons, 2001)], short and long plateau offsets [open and closed circle (Kyriazi *et al.*, 1994)], and the initial response to sine wave deflections at different frequencies [squares (Hartings, 2000)] (see Appendix for further detail). Panel (a) quantifies the relationship between cortical response magnitude and thalamic response magnitude. Panel (b) quantifies the relationship between cortical response magnitude and the initial change in thalamic firing synchrony (see text and Appendix).  $r^2$  values are based on all protocols evoking cortical responses > 1 spike/stimulus (dotted lines).

12 years (Simons and Carvell, 1989; Kyriazi *et al.*, 1994; Hartings 2000; Pinto *et al.*, 2000; Bruno and Simons, 2001). Cortical responses are quantified in terms of response magnitude, and thalamic responses are quantified in terms of either response magnitude (Fig. 4a) or the initial change in firing synchrony (Fig. 4b). Response magnitude is measured as the average number of spikes occurring within a 25 ms response window, and the change in firing synchrony is measured as the initial onset slope of the population PSTH [i.e. TC40, see Appendix and Pinto *et al.* (Pinto *et al.*, 2000) for details]. Experimental methods are summarized in Appendix.

These data show that the cortical response is better predicted by the initial change in firing synchrony among thalamic neurons than by thalamic input magnitude. For deflections that evoke strong cortical responses, averaging 1 spike/stimulus, linear regression analysis indicates that cortical responses are poorly correlated with thalamic response magnitude ( $r^2 = 0.03$ ), but strongly correlated with the initial change in firing synchrony ( $r^2 = 0.83$ ). The fact that data points from all deflection protocols are well-fitted by the same regression line suggests that thalamic input timing is the primary determinant of the cortical response, regardless of how or which whisker is deflected. Deflections that evoke <1 spike/stimulus in cortex fall along a slightly different regression line, having a steeper slope, and correspond to thalamic responses that are more dispersed temporally.

Importantly, these results suggest a different approach to the study of neural coding than those based on quantifying the information contained in neural spike trains (Rieke *et al.*, 1997). In our data, both thalamic response magnitude and timing carry information about ON versus OFF whisker deflections (Fig. 4, open symbols). However, it is the processing mechanisms of the circuit receiving the signal (i.e. barrels) that determine which aspects of thalamic activity are most salient (i.e. timing), not consideration of which aspect may contain the most information.

### How Do Barrels Work?

The barrel circuit is a *temporal contrast detector*, responding selectively to rapid changes in firing synchrony among thalamic input neurons. The experimental validation of predictions from both the full and reduced computational models provides strong support for the hypothesis that the thalamocortical response transformation (RFT1–RFT4) emerges from the four basic principles of barrel organization described above. More importantly, it suggests that understanding how these principles function in the models will provide insight into the function of real barrels as well. In this section, we present numerical and theoretical analyses of the reduced model to understand how the principles of barrel organization dynamically interact to render cortical responses sensitive to thalamic input timing. As described above, the barrel's sensitivity to timing can account for differences in cortical ON versus OFF responses (RFT2). Surprisingly, the same underlying mechanisms will also explain the decrease in spontaneous activity (RFT1), the spatial focusing of cortical receptive fields (RFT3) and the emergence of surround inhibition (RFT4).

Our model of barrel function is intentionally constrained to thalamic and cortical responses that are localized both in time (20–25 ms) and space (a single barrel), and is based on experiments involving relatively simple stimuli. Our goal is to establish a foundation upon which to build an understanding of responses to more complex and natural stimuli. Longer-lasting responses are likely also to require consideration of short-term synaptic modification (Abbott *et al.* 1997; Gil *et al.*, 1997) and cortico-

thalamic feedback (Yuan *et al.*, 1986; Deschenes *et al.*, 1998), in addition to the local circuit dynamics explored here. Responses in laminae other than layer IV are explored below.

### Phase Plane Analysis of Barrel Responses

An advantage of the simple form of the reduced model is that the network's dynamics can be understood visually using a state diagram called a *phase plane* (Fig. 5). On the phase plane, the state of the network at each given moment is defined as the level of activity in the excitatory ( $E$ ) and inhibitory ( $I$ ) populations, represented on the  $x$ - and  $y$ -axes respectively. For each possible state, the values of  $dE/dt$  and  $dI/dt$  (Fig. 2d) quantify the combined influence of intracortical connections and thalamic input on activity in the excitatory and inhibitory populations, respectively. Because the barrel's output is generally represented by activity in the excitatory population ( $E$ ), we use the color axis on the phase plane to present values of  $dE/dt$ . States in which activity in the excitatory population is increasing ( $dE/dt > 0$ , e.g. red region) are separated from states in which it is decreasing ( $dE/dt < 0$ , e.g. blue region) by the line of zero change called the excitatory nullcline (red-brown line). The inhibitory nullcline is defined similarly (gray line). The intersection of the two nullclines ( $dE/dt = dI/dt = 0$ ) corresponds to the steady-state or resting level of activity in the network.

In response to thalamic input, both the nullclines and the color map shift upward as the network's state is displaced from rest. The network's response then evolves according to changing values of  $dE/dt$  and  $dI/dt$ . The response is tracked over time using a *response trajectory* (Fig. 5d,e; black curves). Successive phase planes represent snapshots of the network's dynamics at different time points along the changing thalamic input levels, indicated by the small roman numerals (Fig. 5b). The head of the trajectory (red arrow) marks the network's current state, which changes according to the dynamics of the corresponding phase plane, while the black tail represents prior states. This treatment of the phase plane differs from standard approaches (Rinzel and Ermentrout, 1998) in that the use of time-varying input requires consideration of both the network's state (red arrow) and the influence of intracortical and thalamic connections (color map) as they both vary continuously in time.

To understand the model's sensitivity to thalamic input timing, we first examine the response to a change in thalamic activity that occurs gradually over several seconds. In the limit, this is equivalent to evaluating the network's steady-state response to different levels of tonic input (cf. Fig. 7c). Figure 5a presents overlaid excitatory and inhibitory nullclines from the phaseplane with low and high levels of tonic thalamic activity. As the tonic level of thalamic input increases, the inhibitory nullcline shifts upward to a greater extent than the excitatory nullcline so that their intersection moves upward and to the left. This corresponds to a cortical resting state with less excitatory but more inhibitory activity (i.e. 'inhibitory tone'). Intuitively, this occurs because (i) feedforward inhibition ( $ti$ ) is stronger than feedforward excitation ( $te$ ), and (ii) inhibitory neurons are more responsive to weak input than excitatory neurons. If the change in thalamic activity is sufficiently slow, the network's state will track the nullclines' intersection almost perfectly until both arrive at the new resting level (red arrow). The effect of dominant feedforward inhibition in the barrel system has been verified experimentally in that increased tonic activity in the thalamus is accompanied by increased tonic activity among inhibitory barrel neurons; tonic activity among excitatory barrel neurons, already low, is relatively unchanged (Brumberg *et al.*, 1996). Conversely, trimming the eight surrounding whiskers in

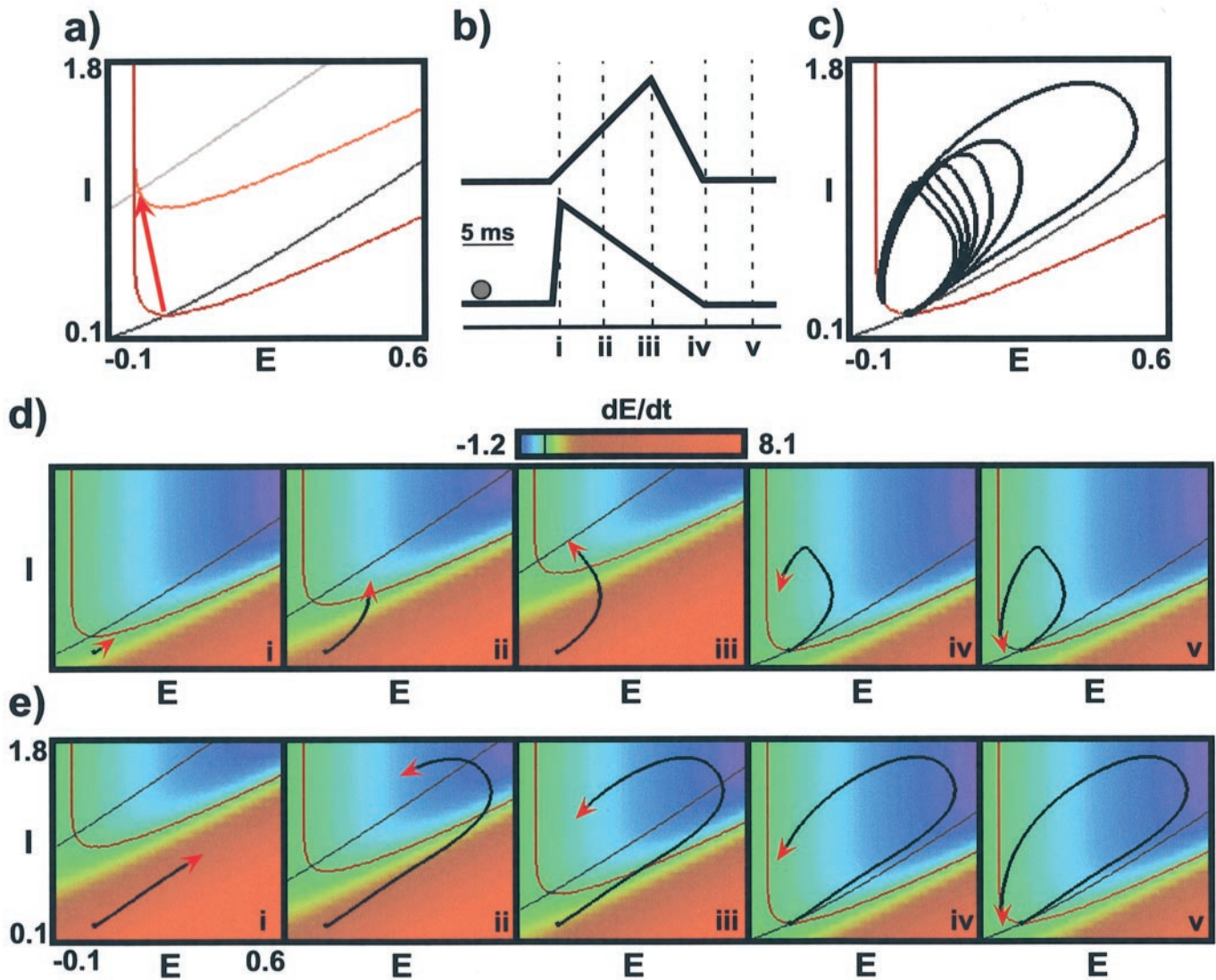


**Figure 5.** Phase plane analysis of barrel responses. Panel (a) shows a phaseplane of the barrel circuit with overlaid excitatory (red-brown lines) and inhibitory (gray lines) nullclines in response to low (dark nullclines) and high (light nullclines) levels of tonic thalamic activity. The large red arrow tracks the course of the response as the input activity changes gradually. Panel (b) shows the slowly (upper) and rapidly (lower) rising simulated thalamic input triangles used to evoke responses shown in panels (d) and (e), respectively. Triangles have a base of 15 ms, peak height of 35 spikes/ms, background activity levels of 0.04 spikes/ms and a time-to-peak of 2 and 10 ms for the rapidly and slowly rising triangles, respectively. The gray dot tracks the same stimulus through previous and later figures. Panel (c) shows overlaid final panels of the phase plane, as in panel v of (d) and (e), in response to a series of input triangles, as in (b), with times-to-peak ranging from 2 to 10 ms. The nullclines in panel (c) represent the state of the network at the end of the response. Panels (d) and (e) present successive phase planes tracking the network's activity and dynamics at time points corresponding to the small roman numerals along the inputs shown in (b). The network's activity is indicated by the black response trajectory. The head of the trajectory (red arrow) marks the network's current state, while the black tail represents prior states. The color indicates how activity in the excitatory population ( $E$ ) changes under the influence of thalamic input and intracortical connections (i.e. the value of  $dE/dt$  in Fig. 2d).

behaving rats decreases activity levels in the thalamus and, as a result of disinhibition, increases activity among excitatory neurons of the cortical barrel corresponding to the spared central whisker (Kelly *et al.*, 1999).

Analysis of the barrel network's steady-state responses provides a basis for understanding its sensitivity to input timing. Figure 5d,e present successive phase planes showing the evolution of the network's response to the slowly and rapidly rising simulated input triangles shown in the upper and lower panels of Figure 5b, respectively. The position of the nullclines prior to the onset of the input triangles is indicated by the lower dark nullclines in Figure 5a; their position when thalamic input reaches its peak value is indicated by the upper light nullclines. The slowly and rapidly rising inputs reach the same peak value, but

in 10 ms (Fig. 5d, panel iii) and 2 ms (Fig. 5e, panel i), respectively. The sensitivity of the network's response to input timing is underscored by the fact that the gradual (Fig. 5a), slow (Fig. 5d) and fast changing (Fig. 5e) thalamic inputs all reach the same peak value but evoke markedly different cortical responses.

Beginning from the initial rest state, thalamic input shifts the nullclines upward. The network's state is then below the nullclines, where thalamic input and network dynamics act to increase activity in both excitatory and inhibitory populations ( $dE/dt > 0$ ,  $dI/dt > 0$ ). For the slowly rising input, the network's state remains relatively close to the nullclines so that activity in both populations is subject to little change ( $dE/dt \approx 0$ ,  $dI/dt \approx 0$ ) (Fig. 5d, panel i). However, because feedforward inhibition is strong (hence the inhibitory nullcline shifts upward further),

inhibition increases to a greater extent than excitation. As a result, the response trajectory quickly overtakes the excitatory nullcline (Fig. 5*d*, panel ii), placing the network in a state where activity in the excitatory population is diminishing. When the peak level of thalamic input finally arrives (Fig. 5*d*, panel iii), the network is already dominated by inhibition ( $dE/dt < 0$ ,  $I > 0$ ), precluding a strong excitatory response.

For the rapidly rising input, the nullclines rise swiftly, placing the network's state far from the nullclines (Fig. 5*e*, panel ii). Note that the rate of increase in excitatory activity ( $dE/dt$ ) grows exponentially with the distance of the network's state from the excitatory nullcline, reflecting the nonlinear effects of recurrent excitation. Thus, in contrast to the slowly rising input, the network's state encounters regions on the phase plane where activity is strongly increasing under the influence of recurrent excitation ( $dE/dt \gg 0$ ). This is because, for the rapidly rising input, the peak level of thalamic input arrives early, when inhibition is still near background levels, and the momentary absence of strong inhibition enables the development of a large excitatory response (Fig. 5*e*, panel ii). Activity in the inhibitory population also increases due to thalamic input and now also in response to the effects of recurrent excitation (via *ei*) (Fig. 5*e*, panels i,ii). Thus, the rapidly rising input evokes the strongest response from both the excitatory and inhibitory populations. Eventually, the trajectory overtakes the excitatory nullcline (Fig. 5*e*, panel ii), and the response tracks the nullclines' intersection back to the original rest state (panels iii-v).

These and other analyses (see Pinto *et al.*, 1996) lead to the following description of how the circuit 'works'. In response to a 'preferred' stimulus, e.g. deflection of the PW, many thalamic neurons discharge at least one spike at short latency. This is represented in the thalamic population PSTH as a rapidly rising increase in activity. Excitatory barrel neurons respond to the synchronous input (Fig. 5*e*, panel i), and reinforce each others' activity nonlinearly ( $dE/dt > 0$ ) via positive feedback provided by recurrent excitation (*ee*). Within a few milliseconds, the non-linear increase in activity is transferred, via *ei* connections, to the inhibitory population (Fig. 5*e*, panel ii), which otherwise responds relatively linearly to thalamic input signals (via *ti*). Now powerfully engaged by both thalamic and local excitatory populations, intrabarrel inhibition overwhelms the excitatory response (via *ie*) and forces the network back to its rest state (Fig. 5*e*, panels iii-v). Thus, even if individual thalamic neurons fire only a single spike to a stimulus, their population effects on barrel neurons can be powerful and rapid, provided that many thalamic neurons fire synchronously and early. On the other hand, when thalamic spikes are temporally dispersed, e.g. following deflections of an AW, the strongly responsive inhibitory cells are more likely to fire than the less responsive excitatory cells. Early on, inhibition dominates the circuit (Fig. 5*d*, panel i), strongly limiting all responses to later arriving thalamic spikes, regardless of their synchrony or number (e.g. Fig. 5*d*, panels ii-iii).

Thus it is the strength of feedforward inhibition and the greater responsiveness of inhibitory neurons to weak, asynchronous inputs that establishes the circuit's sensitivity to input timing. The dominance of inhibition allows only a brief *window of opportunity* for synchronous thalamic inputs to engage positive feedback mechanisms within the barrel circuit, enabling the development of an excitatory response that can momentarily withstand the effects of strong feedforward and feedback inhibition. The circuit's sensitivity to input timing is further illustrated in Figure 5*c*, which presents overlaid final panels of responses on the phase plane to a series of input triangles, all

having the same magnitude but systematically varied in rate of onset.

### Thalamocortical Response Transformation

The phase plane effectively illustrates how the thalamocortical response transformation emerges from the four principles of barrel organization described above. First, the intrinsic nonlinearities distinct to each of the two populations define the shape and orientation of the excitatory and inhibitory nullclines and contribute to the rate at which each population responds to thalamic input. Second, monosynaptic thalamic input onto both populations contributes to the motion of the nullclines over the course of the input signal. Third, the network of synaptic connections among and between the populations contributes to the spatial relationship between the two nullclines and to the sign and value of  $dE/dt$  and  $dI/dt$  throughout phase space. Fourth, the responsiveness of inhibitory neurons contributes to the topology of phase space and establishes the dominance of feedforward and feedback inhibition.

The mechanism that accounts for the model's sensitivity to rapidly versus slowly rising inputs is sufficient to explain all aspects of the thalamocortical response transformation as defined previously. For instance, the larger ON versus OFF (RFT2) and the larger PW versus AW (RFT3) responses can both be explained directly in terms of the barrel's sensitivity to input timing. ON and PW deflections generate rapidly rising population thalamic inputs, whereas OFF and AW deflections generate slowly rising thalamic inputs. At the extreme, as seen in Figure 5*a,d*, very slowly changing inputs evoke inhibition but little excitation. This is precisely what is observed experimentally for the AW and other deflections that evoke temporally dispersed thalamic responses, as shown in Figure 4*b* (see also Fig. 1). The same mechanism accounts for the low level of background activity among excitatory barrel neurons as explained above (RFT1). Interestingly, these results imply that (i) the *spatial* focusing of excitatory receptive fields between thalamus and cortex results from the barrel's sensitivity to input *timing*, and (ii) distinguishing a low-velocity PW deflection from a high-velocity AW deflection (for example) should require integration of information from more than a single barrel-related cortical column, perhaps in the superficial or deep cortical layers (see below).

The emergence of surround inhibition (RFT4) can also be understood in terms of strong feedforward inhibition. Intuitively, as described above for the slowly rising input, AW deflections evoke inhibitory activity in the cortex that effectively suppresses subsequent responses to PW deflections. Moreover, the model also suggests that the strength of surround inhibition should depend on the interval between the AW and PW deflections, which is precisely what is found experimentally (Simons and Carvell, 1989).

### Recurrent Excitation in Damping Networks

Recurrent excitation plays an important role in enhancing the network's response to 'preferred' (rapidly rising) input versus 'non-preferred' (slowly rising) input. On the phase plane, strengthening recurrent excitation (*ee*) increases the rate of exponential growth of activity in the excitatory population as the network's state moves further from the nullclines. As explained above, the initial displacement of the network's state from the nullclines' intersection is greater for inputs with high initial synchrony. Thus, increasing recurrent excitation selectively enhances the network's response to initially synchronous inputs. This is demonstrated directly in Figure 6*a* which presents

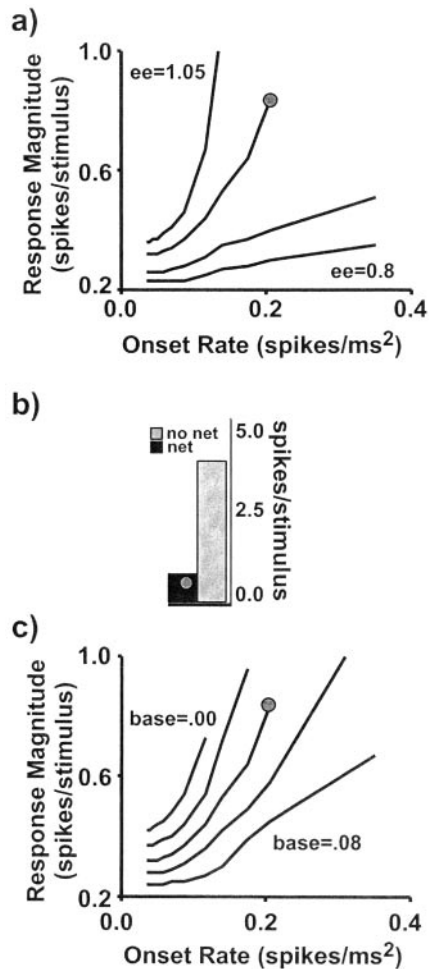


**Figure 6.** Recurrent excitation in damping circuits. Panel (a) shows network responses to input triangles having a base of 15 ms, height of 0.35 spikes/ms, background activity levels of 0.04 spikes/ms, and times-to-peak ranging from 1 to 10 ms. Curves correspond to responses of networks with recurrent excitation ( $ee$ ) of 1.05, 1.0, 0.9 and 0.8, respectively. Panel (b) shows the network's response with network connections set at strengths used to simulate barrel responses (net) and with network connections removed (no net;  $ee, ei, ie, ij = 0$ ). Panel (c) presents network responses generated using the same input triangles as in (a) but with  $ee = 1.0$  and thalamic background activity levels (base) of 0.00, 0.02, 0.04, 0.06 and 0.08 spikes/ms. The gray dot tracks the same stimulus through each panel and previous figures.

responses of the model network with different levels of recurrent excitation to simulated input triangles having the same magnitude but different onset rates (as in Fig. 3c). There is a greater difference between the responses to rapidly versus slowly rising inputs when recurrent excitation is strong.

Previous modeling studies of visual cortical circuitry are based on the idea that recurrent excitation enhances response selectivity by *amplifying* responses to preferred stimuli. That is, when intracortical connections are removed, simulated responses to preferred inputs are reduced relative to when the network is intact (Douglas and Martin, 1991; Somers *et al.*, 1995; Suarez *et al.*, 1995; Adorjan *et al.*, 1999). By contrast, the dominance of inhibition in the barrel circuit renders the overall effect of cortical connections *damping* rather than amplifying. That is, as shown in Figure 6b, when intracortical connections are removed, simulated responses to preferred inputs are enhanced relative to when the network is intact, even when recurrent excitation is strong.

The distinction between damping and amplification may have

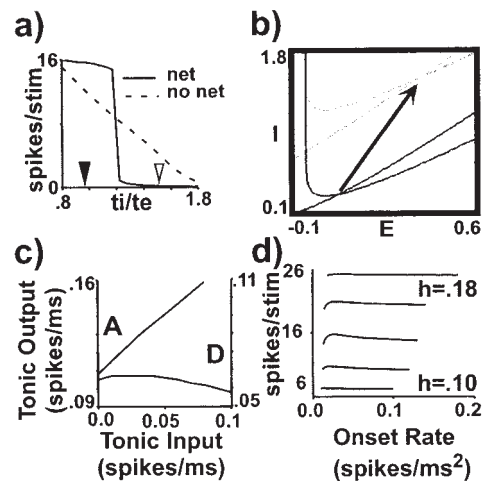


**Figure 7.** Cortical damping versus amplification. Panel (a) shows the magnitude of the network's response as the ratio of  $ti/te$  is changed, both with (net) and without (no net) intracortical connections, as in Figure 6b. The stimulus was the same as indicated by the gray dot in previous figures. Closed and open arrows indicate levels of  $ti/te$  for the phase planes presented in panel (b) and Figure 5a, respectively. Panel (b) shows a phase plane of the amplifying circuit with overlaid nullclines, as in Figure 5a, in response to low (dark) and high (light) levels of tonic thalamic activity. Panel (c) quantifies the steady-state level of activity in the excitatory population in the damping (D, right axis) and amplifying (A, left axis) circuit, in response to increasing levels of tonic thalamic activity. Panel (d) quantifies an amplifying circuit's response to a battery of input triangles having a 15 ms base, times-to-peak ranging from 1 to 10 ms, and heights ( $h$ ) ranging from 0.10 to 0.18 spikes/ms in 0.02 increments. Lines connect responses to input having the same height but different rates of onset. Parameters were adjusted and smaller triangles were used for the amplifying circuit in (c) and (d) to increase the response range and to avoid saturation (see Appendix).

important implications for a circuit's operational characteristics. For instance, data from both visual (Sclar and Freeman, 1982; Skottun *et al.*, 1987) and somatosensory (Brumberg *et al.*, 1996) cortex suggest that real cortical circuits maintain their sensitivities to preferred versus non-preferred stimuli over a wide range of signal-to-background ratios. Responses presented in Figure 6c demonstrate that the sensitivity of simulated barrel responses to input timing are also relatively unaffected by increased levels of thalamic background activity. This is because strong network inhibition suppresses the excitatory populations response to tonic input (see Fig. 5a), endowing the circuit with an intrinsic mechanism for contrast-gain control.

The equations of the reduced barrel model represent an *excitable system* (see Appendix). With different parameter values, an excitable system can be made to function as a damper, like the barrel circuit, or as an amplifier. One way to effect this change is to decrease the strength of feedforward inhibition ( $ti$ ) relative to feedforward excitation ( $te$ ). In particular, Figure 7a shows that changing the balance of feedforward inhibition over excitation ( $ti/te$ ) shifts the network from functioning as a damper, in which removing network connections results in larger responses, to an amplifier, in which removing network connections results in smaller responses. The effect is further illustrated on the phase plane, presented in Figure 7b, which shows excitatory and inhibitory nullclines resulting from low and high levels of tonic thalamic activity, respectively. In comparison with Figure 5a, however, feedforward excitation ( $te$ ) is set to be stronger than feedforward inhibition ( $ti$ ). This causes the excitatory nullcline to rise farther than the inhibitory nullcline so that their intersection moves upward and to the *right*, resulting in a cortical resting state with more excitatory

background activity. Correspondingly, as shown in Figure 7c, amplifying circuits respond strongly to increased levels of thalamic background activity. Beyond a certain point, in fact, amplifying circuits can become unstable and behave as intrinsic oscillators. The responsiveness of amplifying circuits to tonic input leads to response saturation and a loss of tuning (i.e. an 'iceberg effect'; data not shown) which has proven a challenge for many models of visual cortex to overcome [reviewed by Ferster and Miller (Ferster and Miller, 2000)].

Figure 7d presents data suggesting that amplifying circuits may have opposite sensitivities to input timing versus magnitude as damping circuits. In particular, using simulated thalamic input triangles, as in Figure 3c, the responses of the amplifying circuits we tested were highly sensitive to the magnitude of thalamic input but insensitive to the onset rate. This is also consistent with the inability of amplifiers to suppress tonic input as described above.

Further analysis is required for a complete characterization of the functional differences between dampers and amplifiers (see Appendix). However, the response properties presented in Figure 7 are typical for all of the amplifier circuits we examined. Moreover, these data suggest an experimental means by which to identify circuits operating as either dampers or amplifiers. In particular, damping circuits are sensitive to input timing while amplifiers are sensitive to input magnitude. In barrel cortex, the experimentally verified sensitivity to input timing described above, coupled with strong functional and anatomical evidence for the dominance of feedforward inhibition, suggests that barrels function as cortical damping circuits.

## Transformations in the Barrel-related Column

### *Serial and Parallel Processing*

The transformation of thalamic signals by barrel circuitry in layer IV provides a basis for understanding response transformations in other circuits within the barrel-related column. In layer IV, barrels are separated by cell-sparse zones called septa. Septal neurons participate in circuits independent from those of barrels, forming synaptic connections in layer IV largely with other septal neurons (Kim and Ebner, 1999). The response properties of septal neurons are similar to those of thalamic neurons (Brumberg *et al.*, 1999). Interestingly, septal neuron response properties can be captured qualitatively by the reduced model if intracortical connection strengths are reduced by half (data not shown).

In layers superficial to the barrels (layers II/III), excitatory neurons exhibit prolonged responses to both ON and OFF whisker deflections (Brumberg *et al.*, 1999), possibly reflecting a high density of NMDA synapses (Monaghan and Cotman, 1985; Rema and Ebner, 1996). Neurons deep to the barrel layer (layers V/VI) often exhibit more complex and dynamic response properties; some are activated only when particular whiskers are deflected in a unique sequence (Simons, 1985) and/or exhibit multiwhisker receptive fields that evolve over tens of milliseconds [reviewed by Ghazanfar and Nicolelis (Ghazanfar and Nicolelis, 2001)]. Neurons in both the superficial and deep layers exhibit multiwhisker receptive fields (Simons, 1985; Brumberg *et al.*, 1999), possibly reflecting the convergence of signals from multiple barrels (Chapin, 1986).

Evidence suggests that processing within the barrel-related column occurs along both serial and parallel pathways. Signals from the thalamus arrive simultaneously in both barrels and septa, and are processed independently within the two networks. Outputs from layer IV converge onto multiple networks

in the superficial and deep layers (see below), although the neurons of layer V also receive some direct thalamic input (Agmon and Connors, 1991; Gil *et al.*, 1999). This processing model is consistent with response latency measurements in which thalamic activation evokes responses first in layer IV, followed by deep and then superficial cortical layers (Carvell and Simons, 1988; Moore and Nelson, 1998; Brumberg *et al.*, 1999).

### *Multiple Codes in the Cortical Column?*

The damping dynamics of the barrel circuit render it more sensitive to the timing of thalamic input than to thalamic input magnitude. Thus, even though information about whisker deflection parameters (e.g. AW versus PW) is contained in both the timing and magnitude of the thalamic response, it is only the former that is 'decoded' by barrel circuitry. Stated differently, the saliency of an afferent code is determined by the dynamics of the circuitry that receives it. In this regard it may be significant that information about whisker deflection parameters is represented in the output of excitatory barrel neurons by at least three 'codes': population firing synchrony, population response magnitude and response magnitude of individual neurons (Pinto *et al.*, 2000). The multiplicity of codes generated by barrel circuitry suggests that there may be multiple circuits elsewhere in the cortical column, each sensitive to a different code contained in the barrel's output.

Is there evidence for such circuits? The response properties of excitatory barrel neurons are consistently more homogeneous than those of neurons in the thalamus (Simons and Carvell, 1989; Kyriazi *et al.*, 1994; Brumberg *et al.*, 1996, 1999; Pinto *et al.*, 2000). This homogeneity probably reflects the convergence of common input from the thalamus and the strong influence that barrel neurons have on each other's activity by means of their shared circuitry. In contrast, the response properties of neurons in both superficial and deep layers are markedly more heterogeneous than those in the layer IV barrel (Simons, 1978, 1985; Kyriazi *et al.*, 1998; Brumberg *et al.*, 1999). In part, this reflects the more diverse thalamic, columnar, and long-distance cortico-cortical inputs to these layers (Harvey, 1980; Crandall *et al.*, 1986; Grieve and Sillito, 1995). It also suggests, however, the existence of multiple, anatomically intermingled circuits, each having distinct inputs, distinct shared circuits and distinct outputs. Determining how these circuits 'work' will require an understanding not only of their inputs, from the barrels and elsewhere, but also of their intrinsic dynamics.

## Appendix

### *Physiology and Stimulation Protocols*

Details of the experimental methods have been described previously and were similar for all studies from which data were obtained (Simons and Carvell, 1989; Kyriazi *et al.*, 1994; Hartings, 2000; Pinto *et al.*, 2000; Bruno and Simons, 2001). Briefly, adult female rats (Sprague-Dawley strain) were anesthetized for surgical procedures using either Halothane or pentobarbital sodium (Nembutal). Following surgery, anesthesia was discontinued for neuronal recordings, rats were lightly narcotized and sedated by steady infusion of fentanyl (Sublimaze, Janssen Pharmaceuticals; 5–10 µg/kg/h), immobilized with gallamine and/or pancuronium bromide, and artificially respired using a positive pressure respirator. Extracellular single-unit recordings were obtained from either cortical barrel or thalamic ventroposterior medial nucleus neurons using either glass micropipettes filled with 3 M NaCl (Simons and Land, 1987) or tungsten microelectrodes. The standard stimulus deflection waveform was a ramp-and-hold trapezoid producing a 1 mm deflection of 200 ms duration with onset and offset velocities of 135 mm/s. This stimulus was used to determine the units' preferred direction, i.e. the angle evoking

the most spikes, by deflecting the whisker in eight directions spanning 360° in 45° increments.

In Figure 4, the ON and short plateau OFF data (open symbols) are averaged from 64 thalamic neurons and 68 excitatory cortical neurons in response to all eight deflection angles of the PW using the standard stimulus (Kyriazi *et al.*, 1994). The long plateau OFF response (closed circle) was obtained similarly, but with a deflection plateau of 1400 ms duration (Kyriazi *et al.*, 1994). The AW data (closed diamond) were averaged from 42 thalamic and 33 excitatory cortical neurons in response to deflection onset of an AW in the unit's best direction using the standard stimulus (Simons and Carvell, 1989; Bruno and Simons, 2001). The velocity and amplitude data were averaged from 63 thalamic neurons and 40 excitatory cortical neurons in response to deflection onset of the PW in both the preferred direction (down triangles) and caudally (up triangles). The standard stimulus was modified to produce whisker deflections that varied over five velocities (210, 170, 145, 130, 70 mm/s) and three amplitudes (7.4°/650 μm, 4.5°/390 μm, 2.6°/225 μm) (Pinto *et al.*, 2000). The sine wave frequency data (squares) were averaged from 22 excitatory cortical neurons and 27 thalamic neurons in response to deflection of the PW in the preferred direction using sinusoidal waveforms with a peak deflection amplitude of 1 mm and frequencies of 4, 8, 10, 12, 16, 20, 30 and 40 Hz; responses beyond the first quarter-cycle (i.e. the initial rise) were not considered in the present study (Hartings, 2000).

#### Analysis of Experimental Data

Spike data were accumulated into PSTHs with a binwidth of 100 μs and summed over each sampled population. Responses were measured from spikes occurring within a 25 ms response window beginning with the initial rise above baseline of the population response. Two response measures were calculated. Response magnitude is measured as the average number of spikes comprising the PSTH over the 25 ms response window. The initial change in firing synchrony is calculated as 40% of the response magnitude divided by the time required to generate the first 40% of the response; this approximates the initial slope of the population PSTH (TC40) [further details are given by Pinto *et al.* (Pinto *et al.*, 2000)].

#### Modeling and Analysis

Details of the reduced model and its construction have been previously described (Pinto *et al.*, 1996). Activity in the excitatory ( $E$ ) and inhibitory ( $I$ ) population is computed according to the following equations, which are similar in form to those described by Wilson and Cowan (Wilson and Cowan, 1972):

$$\tau_c \frac{dE}{dt} + E = P_c(ee E - ie I + te T)$$

$$\tau_i \frac{dI}{dt} + I = P_i(ei E - ii I + ti T)$$

Activity in each population (e.g. excitatory) is measured in units of synaptic drive ( $E$ ), firing rate ( $P_c$ ), and voltage (the argument of  $P_c$ ) [for a full discussion see Pinto *et al.* (Pinto *et al.* 1996)]. Parameter values were chosen as follows to reproduce barrel population responses to whisker deflection onset and offset (Pinto *et al.*, 1996):  $\tau_c = 5$  (ms),  $\tau_i = 15$ ,  $ee = 42.0$ ,  $ei = 42$ ,  $ie = 25$ ,  $ii = 18$ ,  $te = 47$ ,  $ti = 60$ ,  $P_c = \gamma_c[1 + \text{erf}[V - (\theta - \rho)/\text{etemp}]]/2$ , where  $\text{erf}(x) = (2/\sqrt{\pi}) \int \exp(-y^2)dy$ ,  $\theta = 0.45$ ,  $\rho = -0.60$ ,  $\text{etemp} = 10.21$ ,  $\gamma_c = 5.12$ .  $P_i$  is the same except  $\text{itemp} = 9.65$ ,  $\gamma_i = 11.61$ . In the reduced model, population synaptic strengths are the product of individual synaptic strengths and convergence factors from the full model, e.g.  $ee = ec w_{ei}$ ,  $ec = 42$ ,  $ic = 12$ ,  $tce = 12$ ,  $tci = 10$ ,  $w_{ce} = 1.0$ ,  $w_{ei} = 1.0$ ,  $w_{ic} = 2.0$ ,  $w_{ii} = 1.5$ ,  $w_{ic} = 3.9$ ,  $w_{ii} = 6.0$ . The parameter values for the amplifying circuit used in Figure 8a,b are the same as the barrel circuit except  $w_{ic} = 5.4$ ,  $w_{ii} = 4.6$ . The parameter values for the amplifying circuit were modified for Figure 7c,d to increase the circuit's response range and to avoid saturation:  $\tau_e = 5$ ,  $\tau_i = 15$ ,  $ee = 76$ ,  $ei = 71$ ,  $ie = 26$ ,  $ii = 18$ ,  $te = 39$ ,  $ti = 60$ ,  $P_c$  and  $P_i$  are as above except  $\gamma_c = 1.0$ ,  $\gamma_i = 2.0$ ,  $\text{etemp} = 15.47$ ,  $\text{itemp} = 14.67$ . All amplifying circuits we examined produced qualitatively similar results.

Differences in parameter values from those previously published (Pinto *et al.*, 1996) reflect the exclusion of refractory terms from the Wilson-Cowan formulation and the use of a fourth-order Runge-Kutta method to solve the equations numerically. In the reduced model, the

time constant for the excitatory population is set shorter than for the inhibitory population, which may appear to contradict the fact that inhibitory neurons are known to have faster membrane time constants (McCormick *et al.*, 1985; Gibson *et al.*, 1999). However, the formulation of the equations indicates that  $\tau_e$  and  $\tau_i$  represent synaptic decay rates, not membrane time constants [reviewed by Ermentrout (Ermentrout, 1998)].

Thalamic population inputs ( $T$ ) were either simulated or constructed from PSTHs obtained previously from *in vivo* single-unit recordings of thalamic neurons (Simons and Carvell, 1989; Kyriazi *et al.*, 1994). Simulated inputs consist of input triangles with a 15 ms base and background firing rates of 0.04 spikes/ms unless otherwise specified. Input triangles varied in times-to-peak from 1 to 10 ms, with heights as specified in the figure legends. The triangles' onset rate is calculated as the height divided by the time-to-peak. Experimentally obtained PSTHs were 'synaptically' filtered using the following equation to generate a measure of thalamic synaptic drive compatible with the variables  $E$  and  $I$  (Pinto *et al.*, 1996):

$$\tau_c \frac{dT}{dt} + T = PSTH$$

Phase planes and simulated response measures were obtained numerically using the XPP (G. Bard Ermentrout, [www.pitt.edu/~phase](http://www.pitt.edu/~phase)) and Maple VR5 (Waterloo Software, Ontario, Canada) software packages. On the phase plane, activity is represented in units of synaptic drive. Otherwise, response magnitudes are measured in spikes/stimulus, the integral of the firing rate in the excitatory population ( $P_c$ ) over the duration of the evoked response. Fixed durations were established to allow sufficient time for activity to return to rest (25 ms for the damper, 50 ms for the amplifier). Interestingly, phase plane analysis suggests that the reduced model is a Type II excitable system (Rinzel and Ermentrout, 1998), and that inputs are either damped or amplified depending on whether they evoke sub- or suprathreshold responses from the circuit. In the context of the barrel system, suprathreshold events, which consist of self-sustained responses often lasting hundreds of milliseconds, may represent epileptiform discharges that occur in diseased or injured states producing hyperexcitable tissue.

The reduced model, input files, parameter sets and phase plane animations are available at the Barrels Web online (<http://www.neurobio.pitt.edu/barrels>).

#### Notes

\*D.J.P. and J.A.H. contributed equally to this work.

The authors wish to thank Bard Ermentrout for useful discussions during the early stages of this work and Randy Bruno for the use of adjacent whisker response data. This work was supported by NIH NS25983, DA12500 (D.J.P.), NIMH K01-MH01944-01A1 (J.C.B.), NIH NS19950 (D.J.S.). Previous modeling and experimental work was supported by NSF IBN421380.

Address correspondence to David J. Pinto, Box 1953, Department of Neuroscience, Brown University, Providence, RI 02912, USA. Email: [dpinto@bu.edu](mailto:dpinto@bu.edu).

#### References

- Abbott LF, Varela JA, Sen K, Nelson SB (1997) Synaptic depression and cortical gain control. *Science* 275:220-224.
- Adorjan P, Levitt JB, Lund JS, Obermayer K (1999) A model for the intracortical origin of orientation preference and tuning in macaque striate cortex. *Vis Neurosci* 16:303-318.
- Agmon A, Connors BW (1991) Thalamic cortical responses of mouse somatosensory (barrel) cortex *in vitro*. *Neuroscience* 41:365-379.
- Ahmed BA, Anderson JC, Douglas RJ, Martin KAC, Nelson JC (1994) Polynuclear innervation of spiny stellate neurons in cat visual cortex. *J Comp Neurol* 341:39-49.
- Angulo MC, Rossier J, Audinat E (1999) Postsynaptic glutamate receptors and integrative properties of fast-spiking interneurons in the rat neocortex. *J Neurophysiol* 82:1295-1302.
- Benshalom G, White EJ (1986) Quantification of thalamocortical synapses with spiny stellate neurons in layer IV of mouse somatosensory cortex. *J Comp Neurol* 253:303-314.
- Ben-Yishai R, Lev Bar-Or R, Sompolinsky H (1995) Theory of orientation tuning in visual cortex. *Proc Natl Acad Sci USA* 92:3844-3848.

- Bruno RM, Simons DJ (2001) Mechanisms of feedforward inhibition in thalamocortical circuits of the rat whisker/barrel system. *Soc Neurosci Abstr* 27:393.
- Brumberg JC, Pinto DJ, Simons DJ (1996) Spatial gradients and inhibitory summation in the rat whisker barrel system. *J Neurophysiol* 76:130-140.
- Brumberg JC, Pinto DJ, Simons DJ (1999) Cortical columnar processing in the rat whisker-to-barrel system. *J Neurophysiol* 82:1808-1817.
- Calloway EM (1998) Local circuits in primary visual cortex of the macaque monkey. *Annu Rev Neurosci* 21:47-74.
- Carvell GE, Simons DJ (1988) Membrane potential changes in rat Sml cortical neurons evoked by controlled stimulation of mystacial vibrissae. *Brain Res* 448:186-191.
- Chapin JK (1986) Laminar differences in sizes, shapes and response profiles of cutaneous receptive fields in the rat S1 cortex. *Exp Brain Res* 62:549-559.
- Chmielowska J, Carvell GE, Simons DJ (1989) Spatial organization of thalamocortical and corticocortical projection system in the rat Sml barrel cortex. *J Comp Neurol* 285:325-338.
- Crandall JE, Korde M, Caviness VS Jr (1986) Somata of layer V projection neurons in the mouse barrel cortex are in preferential register with the sides and septa of the barrels. *Neurosci Lett* 67:19-24.
- Deschenes M, Veinante P, Zhang ZW (1998) The organization of corticothalamic projections: reciprocity vs. parity. *Brain Res Rev* 28:286-308.
- Douglas RJ and Martin KAC (1991) A functional microcircuit for cat visual cortex. *J Physiol* 440:735-769.
- Douglas RJ, Martin KAC, Whitteridge D (1989) A canonical microcircuit for neocortex. *Neural Comp* 1:480-488.
- Douglas RJ, Koch C, Mahowald M, Martin KAC, Suarez HH (1995) Recurrent excitation in neocortical circuits. *Science* 269:981-985.
- Ermentrout GB (1998) Neural nets as spatio-temporal pattern forming systems. *Rep Prog Physiol* 61:353-430.
- Ferster D, Miller KD (2000) Neural mechanisms of orientation selectivity in the visual cortex. *Annu Rev Neurosci* 23:441-471.
- Ghazanfar AA, Nicolelis MAL (2001) The structure and function of dynamic cortical and thalamic receptive fields. *Cereb Cortex* 11:183-193.
- Gibson J, Beierlein M, Connors B (1999) Two networks of electrically coupled inhibitory neurons in neocortex. *Nature* 402(6757):75-79.
- Gil Z, Connors BW, Amitai Y (1997) Differential regulation of neocortical synapses by neuromodulators and activity. *Neuron* 19:679-686.
- Gil Z, Connors BW, Amitai Y (1999) Efficacy of thalamocortical and corticocortical synaptic connections: quanta, innervation and reliability. *Neuron* 23:385-397.
- Goldreich D, Kyriazi HT, Simons DJ (1999) Functional independence of layer IV barrels in rodent somatosensory cortex. *J Neurophysiol* 82:1311-1316.
- Grieve KL, Sillito AM (1995) Differential properties of cells in the feline primary visual cortex providing the corticofugal feedback to the lateral geniculate nucleus and visual claustrum. *J Neurosci* 15:4868-4874.
- Hartings JA (2000) Somatosensory processing in inhibitory feedback circuits of the thalamus. Ph.D. thesis, University of Pittsburgh.
- Harvey AR (1980) A physiological analysis of subcortical and commissural projections of areas 17 and 18 of the cat. *J Physiol* 302:507-534.
- Hubel DH, Wiesel TN (1962) Receptive fields, binocular interaction and functional architecture in the cat's visual cortex. *J Physiol* 160:106-154.
- Keller A (1995) Synaptic organization of the barrel cortex. In: *Cerebral cortex*, vol. 11: The barrel cortex of rodents (Jones ET, Diamond IT, eds), pp. 221-262. New York: Plenum.
- Kelly MK, Carvell GE, Kodger JM, Simons DJ (1999) Sensory loss by selected whisker removal produces immediate disinhibition in the somatosensory cortex of behaving rats. *J Neurosci* 19:9117-9125.
- Kim U, Ebner FF (1999) Barrels and septa: separate circuits in rat barrel field cortex. *J Comp Neurol* 408:489-505.
- Kyriazi HT, Simons DJ (1993) Thalamocortical response transformations in simulated whisker barrels. *J Neurosci* 13:1601-1615.
- Kyriazi HT, Carvell GE, Simons DJ (1994) OFF Response transformations in the whisker/barrel system. *J Neurophysiol* 72:392-401.
- Kyriazi HT, Carvell GE, Brumberg JC, Simons DJ (1996) Quantitative effects of GABA and bicuculline methiodide on receptive field properties of neurons in real and simulated whisker barrels. *J Neurophysiol* 75:547-560.
- Kyriazi HT, Carvell GE, Brumberg JC, Simons DJ (1998) Laminar differences in bicuculline methiodide's effect on cortical neurons in the rat whisker barrel system. *Somatosens Mot Res* 15:146-156.
- McCasland JS and Hibbard LS (1997) GABAergic neurons in barrel cortex show strong, whisker-dependent metabolic activation during normal behavior. *J Neurosci* 17:5509-5527.
- McCormick DA, Connors BW, Lighthall JW, and Prince DA (1985) Comparative electrophysiology of pyramidal and sparsely spiny stellate neurons of the neocortex. *J Neurophysiol* 54:782-806.
- Miller KD, Pinto DJ, Simons DJ (2001) Processing in layer 4 of the neocortical circuit: new insights from visual and somatosensory cortex. *Curr Opin Neurobiol* 11:488-497.
- Monaghan DT, Cotman CW (1985) Distribution of *N*-methyl-D-aspartate-sensitive L<sup>3</sup>H-glutamate-binding sites in rat brain. *J Neurosci* 5:2909-2919.
- Moore C, Nelson S (1998) Spatio-temporal subthreshold receptive fields in the vibrissa representation of rat primary somatosensory cortex. *J Neurophysiol* 8:2882-2892.
- Petersen CH, Sakmann B (2001) The excitatory neural network of rat layer 4 barrel cortex. *J Neurosci* 20:7579-7586.
- Pinto DJ, Brumberg JC, Simons DJ, Ermentrout GB (1996) A quantitative population model of whisker barrels: re-examining the Wilson-Cowan equations. *J Comput Neurosci* 3:247-264.
- Pinto DJ, Brumberg JC, Simons DJ (2000) Circuit dynamics and coding strategies in rodent somatosensory cortex. *J Neurophysiol* 83:1158-1166.
- Rema V, Ebner FF (1996) Postnatal changes in NMDAR1 subunit expression in the rat trigeminal pathway to barrel field cortex. *J Comp Neurol* 368:165-184.
- Rieke F, Warland D, de Ruyter van Steveninck R, Bialek W (1997) *Spikes: exploring the neural code*. Cambridge, MA: MIT Press.
- Rinzel J, Ermentrout GB (1998) Analysis of neural excitability and oscillations. In: *Methods in neuronal modeling* (Kock C, Segev I, eds), pp. 251-291. Cambridge, MA: MIT Press.
- Sclar G, Freeman RD (1982) Orientation selectivity in the cat's striate cortex is invariant with stimulus contrast. *Exp Brain Res* 46:457-461.
- Shoykhet M, Doherty D, Simons DJ (2000) Coding of deflection velocity and amplitude by whisker primary afferent neurons: implications for higher level processing. *Somatosens Mot Res* 17:171-180.
- Simons DJ (1978) Response properties of vibrissa units in rat SI somatosensory cortex. *J Neurophysiol* 41:198-220.
- Simons DJ (1985) Temporal and spatial integration in the rat SI vibrissa cortex. *J Neurophysiol* 54:615-635.
- Simons DJ (1997) Rodent whisker barrels: windows into cerebral cortical function. *News Physiol Sci* 12:268-273.
- Simons DJ, Carvell GE (1989) Thalamocortical response transformations in the rat vibrissa/barrel system. *J Neurophysiol* 61:611-630.
- Simons DJ, Land PW (1987) A reliable technique for marking the location of extracellular recording sites using glass micropipettes. *Neurosci Lett* 81:100-104.
- Skottun BC, Bradley A, Sclar G, Ohzawa I, Freeman RD (1987) The effects of contrast on visual orientation and spatial frequency discrimination: a comparison of single cells and behavior. *J Neurophysiol* 57:773-786.
- Somers DC, Nelson SB and Sur M (1995) An emergent model of orientation selectivity in cat visual cortical simple cells. *J Neurosci* 15:5448-5465.
- Suarez H, Koch C, Douglas R (1995) Modeling direction selectivity of simple cells in striate visual cortex within the framework of the canonical microcircuit. *J Neurosci* 15:6700-6719.
- Swadlow HA (1995) Influence of VPM afferents on putative inhibitory interneurons in S1 of the awake rabbit: evidence from cross-correlation, microstimulation, and latencies to peripheral sensory stimulation. *J Neurophysiol* 73:1584-1599.
- Swadlow HA, Gusev AG (2000) The influence of single VB thalamocortical impulses on barrel columns of rabbit somatosensory cortex. *J Neurophysiol* 83:2802-2813.
- Temereanca S, Kyriazi HT, Simons DJ (2000) Effects of corticofugal projections on whisker-evoked thalamic response synchrony. *Soc Neurosci Abstr* 26:132.
- Welker C (1971) Microelectrode delineation of fine grain somatotopic organization of Sml cerebral cortex in albino rat. *Brain Res* 26:259-275.
- White EL (1978) Identified neurons in mouse Sml cortex which are postsynaptic to thalamocortical axon terminals: a combined

- Golgi-electron microscopic and degeneration study. *J Comp Neurol* 181:627-661.
- White EL (1989) *Cortical circuits: synaptic organization of the cerebral cortex*. Boston, MA: Birkhauser.
- White EL, DeAmicas RA (1977) Afferent and efferent projections of the region in mouse SmI cortex which contains the posteromedial barrel subfield. *J Comp Neurol* 175:455-481.
- White EL, Rock MP (1980) Three-dimensional aspects and synaptic relationships of a Golgi-impregnated spiny stellate cell reconstruction from serial thin sections. *J Neurocytol* 9:6156-636.
- White EL, Rock MP (1981) A comparison of thalamocortical and other synaptic inputs to dendrites. *J Comp Neurol* 195:265-277.
- Wilson HR, Cowan JD (1972) Excitatory and inhibitory interactions in localized populations of model neurons. *Biophys J* 12:1-24.
- Woolsey TA, Van der Loos H (1970) The structural organization of layer IV in the somatosensory region (SI) of mouse cerebral cortex. *Brain Res* 17:205-242.
- Yuan B, Morrow TJ, Casey KL (1986) Corticofugal influence of SI cortex on ventrobasal thalamic neurons in the awake rat. *J Neurosci* 6:3611-3617.